

Prediction of $B_c \rightarrow D\pi$ in the PQCD approach

Jian-Feng Cheng*

Institute of High Energy Physics, CAS, P.O. Box 918(4), Beijing 100049, China

Dong-Sheng Du and Cai-Dian Lü

*CCAST (World Laboratory), P.O. Box 8730, Beijing 100080, China; and
Institute of High Energy Physics, CAS, P.O. Box 918(4), Beijing 100049, China[†]*

(Dated: October 30, 2018)

We investigate the branching ratios and direct CP asymmetries of $B_c^+ \rightarrow D^0\pi^+$ and $B_c^+ \rightarrow D^+\pi^0$ decays in the PQCD approach. All the diagrams with emission topology or annihilation topology are calculated strictly. A branching ratio of 10^{-6} and 10^{-7} for $B_c^+ \rightarrow D^0\pi^+$ and $B_c^+ \rightarrow D^+\pi^0$ decay is predicted, respectively. Because of the different weak phase and strong phase from penguin operator and two kinds of tree operator contributions, we predict a possible large direct CP violation: $A_{cp}^{\text{dir}}(B_c^\pm \rightarrow D^0\pi^\pm) \approx -50\%$ and $A_{cp}^{\text{dir}}(B_c^\pm \rightarrow D^\pm\pi^0) \approx 25\%$ when $\gamma = 55^\circ$, which can be tested in the coming LHC.

PACS numbers: 13.25.HW, 12.38.Bx

I. INTRODUCTION

The charmless B decays provide a good platform to test the Standard Model (SM) and study the CP violation, which arouses physicists' great interest and has been discussed in the literature widely. But how about the B_c decays, the b quark of which has similar property with that of B meson? There are some events of B_c at Tevatron [1] and will be a great number of events appearing at LHC in the foreseeable future. The progress of the experiments makes us to think of a question: what will be the theoretical prediction on the two-body non-leptonic B_c decays?

Different from B and B_s meson, B_c meson consists of two heavy quarks b and c , which can decay individually. Because of the difference of mass, lifetime and the relative CKM matrix element between b and c quark, the decay rate of the two quarks is different, which determines the unique property of B_c decays. Though c quark's mass is about one third of b quark, leading to a suppression of $(M_c/M_b)^5$, the decay of c quark can not be ignored because the corresponding CKM matrix element V_{cs} is larger than that of b quark: V_{ub}, V_{cb} . Because of the small mass of c quark, the decay of c quark is nearly at non-perturbative scale, where there is great theoretical difficulty. Now we study the b quark decay first and leave the study of c quark decay to the future.

In recent years, a great progress has been made in studying two-body non-leptonic B decays in perturbative QCD approach (PQCD) [2, 3], QCD factorization [4] and soft collinear effective theory (SCET) [5]. Though B_c decay has been studied [6] in Naive Factorization [7, 8] many years ago, no one applies the method developed recently in such processes. In this paper we will use $B_c \rightarrow D\pi$ as an example to discuss the B_c decays in the PQCD approach.

The $B_c \rightarrow D\pi$ decay provides opportunities to study

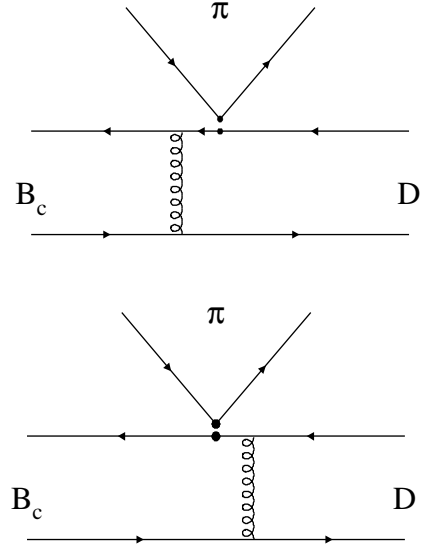


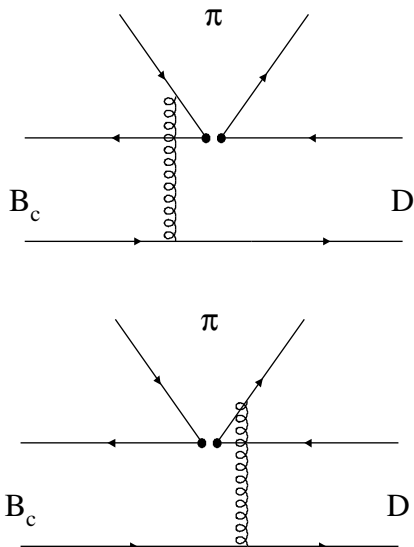
FIG. 1: Form factor in $B_c \rightarrow D\pi$.

the direct CP asymmetry. Different from the B decays [3], $B_c \rightarrow D\pi$ has the direct CP asymmetry even without considering the contributions from penguin operators, because the tree contributions from the annihilation topology provide not only the strong phase, but also the different weak phase. According to the power counting rule of PQCD, the tree contributions from the annihilation topology is power suppressed. But the larger CKM matrix elements $|V_{cb}|$ enhances the contribution to make it larger than the penguin contributions, so the direct CP asymmetry of $B_c \rightarrow D\pi$ can be very large, which is found in our numerical analysis.

The study of B_c decay also provides opportunities to test k_T factorization in PQCD approach. According to numerical analysis in the literature, the form factor contributions from Fig.1 usually dominate the whole decays. In the same way, the form factor also gives the main contributions in the $B_c \rightarrow D\pi$ decay according to our numerical analysis. Since the B_c meson consists of two heavy quarks, the effect of k_T in the B_c meson can be

*Email: chengjf@mail.ihep.ac.cn

[†]Mailing address.

FIG. 2: Non-factorizable emission topology in $B_c \rightarrow D\pi$.

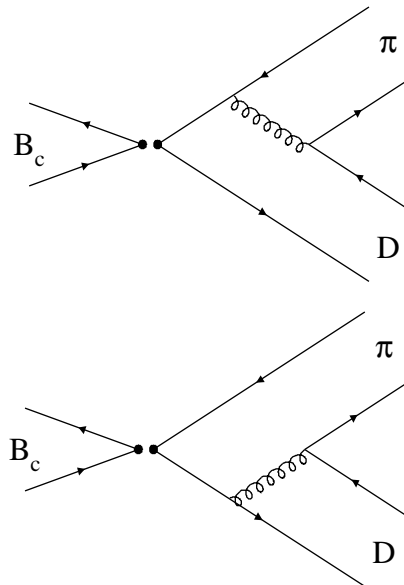
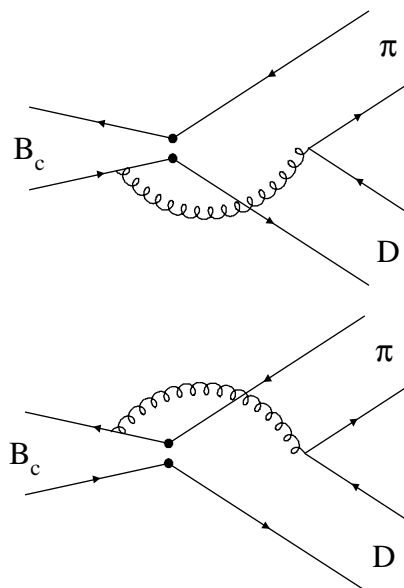
ignored and the form factor $B_c \rightarrow D$ only includes the k_T contributions from D meson. So it is easier to study how important the k_T contributions are in B_c decays than that in the B decays because the latter need to consider both k_T contributions of B and D meson.

The $B_c \rightarrow D\pi$ decay also provides a good platform to study the D meson's wave function. The D meson's mass M_D is not so large that it is hard to get the ideal wave function of D meson by the expansion of $1/M_D$ as in B meson. People use the form fitted from experimental data generally. Such discussion has been done by Ref. [9] in the form factor $B \rightarrow D$ transition. It is better to discuss D meson wave function in $B_c \rightarrow D\pi$ for two reasons: one is that the hierarchy between M_{B_c} and M_D ($M_{B_c} \gg M_D$) guarantees us to apply the k_T factorization theorem in this process, the other is that the wave function of B_c is clean, which eliminates the possible uncertainty from B_c meson. The experiment of B_c decays will test how reasonable it is. As the only parameter with large uncertainty, the wave function of D meson need further theoretical investigation.

II. FRAMEWORK

The hard amplitudes of these decays contain factorizable diagrams (Fig. 1), where hard gluons attach the valence quarks in the same meson, and non-factorizable diagrams (Fig. 2), where hard gluons attach the valence quarks in different mesons. The annihilation topology is also included, and classified into factorizable (Fig. 3) and non-factorizable (Fig. 4) ones according to the above definitions.

In the calculations of all the diagrams, we can ignore the k_T contributions of B_c meson because it consists of two heavy quarks. Furthermore, we can suppose the two quarks \bar{b} and c of B_c^+ meson to be on the mass shell approximately and treat the wave function of B_c meson as δ function for simplicity, so we can integrate the wave

FIG. 3: Factorizable annihilation topology in $B_c \rightarrow D\pi$.FIG. 4: Non-factorizable annihilation topology in $B_c \rightarrow D\pi$.

function B_c out and the k_T factorization form turns into

Form factor

$$\sim \int d^4 k_1 \Phi_D(k_1) C(t) H(k_1, t), \quad (1)$$

Other topology

$$\sim \int d^4 k_1 d^4 k_2 \Phi_D(k_1) \Phi_\pi(k_2) C(t) H(k_1, k_2, t), \quad (2)$$

where $k_{1(2)}$ is momentum of light (anti) quark of $D(\pi)$ meson. The non-factorizable topology includes two kinds of topology: emission topology (Fig. 2) and annihilation topology (Fig. 4). In the above equations, we sum over all Dirac structure and color indices. The hard components consist of the hard part ($H(t)$) and harder dynamics ($C(t)$), the former $H(t)$ can be calculated perturbatively; the latter $C(t)$ is the Wilson coefficients which

runs from electro-weak scale M_W to the lower factorization scale t . Φ_M is the wave function of D and π meson, including the non-perturbative contributions in the k_T factorization.

Through out the paper, we use the light-cone coordinate to describe the meson's momentum in the rest frame of the B_c meson. According to the conservation of four-momentum, we get the momentum of three mesons B_c , D and π up to the order of r_2^2 ($r_2 = M_D/M_{B_c}$) as following:

$$\begin{aligned} P_{B_c} &= \frac{M_{B_c}}{\sqrt{2}}(1, 1, \mathbf{0}_T), \\ P_2 &= \frac{M_{B_c}}{\sqrt{2}}(1, r_2^2, \mathbf{0}_T), \\ P_3 &= \frac{M_{B_c}}{\sqrt{2}}(0, 1 - r_2^2, \mathbf{0}_T), \end{aligned} \quad (3)$$

where we have neglected the small mass of pion and higher order terms of r_2 . Such approximation will be used in the whole paper.

III. CALCULATION OF AMPLITUDES

A. Wave Function

B_c meson consists of two heavy quarks such that the small Λ_{QCD} can be ignored ($\Lambda_{\text{QCD}} = M_{B_c} - M_b - M_c \ll M_c$ or M_b), so as the quark transverse momentum k_T . In principal there are two Lorentz structures in the B or B_c meson wave function. One should consider both of them in calculations. However, it can be argued that one of the contribution is numerically small [10], thus its contribution can be neglected. Therefore, we only consider the contribution of one Lorentz structure, such that we can reduce the number of input parameters

$$\Phi_{B_c}(x) = \frac{i}{4N_c}(\not{x}_{B_c} + M_{B_c})\gamma_5 \delta(x - M_c/M_{B_c}). \quad (4)$$

The other two mesons' wave functions read:

$$\Phi_D(x, b) = \frac{i}{\sqrt{2N_c}}\gamma_5(\not{P}_2 + M_D)\phi_D(x, b), \quad (5)$$

$$\begin{aligned} \Phi_\pi(x) &= \frac{i}{\sqrt{2N_c}}[\gamma_5 \not{P}_3 \phi_\pi(x) + M_{0\pi} \gamma_5 \phi_\pi^p(x) \\ &\quad + M_{0\pi} \gamma_5 (\not{x}_- \not{x}_+ - 1) \phi_\pi^\sigma(x)], \end{aligned} \quad (6)$$

where $N_c = 3$ is color degree of freedom, and $M_{0\pi} = M_\pi^2/(m_u + m_d)$, $n_- = (0, 1, \mathbf{0}_T) \propto P_3$, $n_+ = (1, 0, \mathbf{0}_T)$, $\epsilon^{0123} = 1$.

The momentum fraction of the light quark in the three mesons can be defined as: $x_1 = k_c/P_{B_c}$, $x_2 = k_2^+/P_2^+$, $x_3 = k_3^-/P_3^-$. In the B_c meson, there are also another relation between x_1 and $r_b = M_b/M_{B_c}$: $x_1 + r_b = 1$.

B. Effective Hamiltonian

The effective Hamiltonian for the flavor-changing $b \rightarrow d$ transition is given by [11]

$$H_{\text{eff}} = \frac{G_F}{\sqrt{2}} \sum_{q=u,c} V_q \left[C_1(\mu) O_1^{(q)}(\mu) + C_2(\mu) O_2^{(q)}(\mu) \right. \\ \left. + \sum_{i=3}^{10} C_i(\mu) O_i(\mu) \right], \quad (7)$$

with the Cabibbo-Kobayashi-Maskawa (CKM) matrix elements $V_q = V_{qd}V_{qb}^*$ and the operators

$$\begin{aligned} O_1^{(q)} &= (\bar{d}_i q_j)_{V-A} (\bar{q}_j b_i)_{V-A}, \\ O_2^{(q)} &= (\bar{d}_i q_i)_{V-A} (\bar{q}_j b_j)_{V-A}, \\ O_3 &= (\bar{d}_i b_i)_{V-A} \sum_q (\bar{q}_j q_j)_{V-A}, \\ O_4 &= (\bar{d}_i b_j)_{V-A} \sum_q (\bar{q}_j q_i)_{V-A}, \\ O_5 &= (\bar{d}_i b_i)_{V-A} \sum_q (\bar{q}_j q_j)_{V+A}, \\ O_6 &= (\bar{d}_i b_j)_{V-A} \sum_q (\bar{q}_j q_i)_{V+A}, \\ O_7 &= \frac{3}{2} (\bar{d}_i b_i)_{V-A} \sum_q e_q (\bar{q}_j q_j)_{V+A}, \\ O_8 &= \frac{3}{2} (\bar{d}_i b_j)_{V-A} \sum_q e_q (\bar{q}_j q_i)_{V+A}, \\ O_9 &= \frac{3}{2} (\bar{d}_i b_i)_{V-A} \sum_q e_q (\bar{q}_j q_j)_{V-A}, \\ O_{10} &= \frac{3}{2} (\bar{d}_i b_j)_{V-A} \sum_q e_q (\bar{q}_j q_i)_{V-A}, \end{aligned} \quad (8)$$

with i and j being the color indices. Using the unitary condition, the CKM matrix elements for the penguin operators O_3 - O_{10} can also be expressed as $V_u + V_c = -V_t$.

The $B_c \rightarrow D\pi$ decay rates have the expressions

$$\Gamma = \frac{G_F^2 M_{B_c}^3}{32\pi} |A|^2. \quad (9)$$

The decay amplitude A of $B_c \rightarrow D\pi$ process from all the diagrams can be expressed in the following:

$$\begin{aligned} A_{D^0\pi^+} &= V_u (f_\pi F_{e1}^T + M_{e1}^T) + V_c (f_{B_c} F_a^T + M_a^T) \\ &\quad - V_t (f_\pi F_{e1}^{P1} + f_\pi F_{e1}^{P3} + M_{e1}^{P1} + M_{e1}^{P2}) \\ &\quad + f_{B_c} F_a^{P1} + f_{B_c} F_a^{P3} + M_a^{P1} + M_a^{P2}, \end{aligned} \quad (10)$$

$$\begin{aligned} \sqrt{2} A_{D^+\pi^0} &= V_u (f_\pi F_{e2}^T + M_{e2}^T) - V_c (f_{B_c} F_a^T + M_a^T) \\ &\quad - V_t (f_\pi F_{e2}^{P1} + f_\pi F_{e2}^{P2} + f_\pi F_{e2}^{P3} \\ &\quad + M_{e2}^{P1} + M_{e2}^{P2} + M_{e2}^{P3} - f_{B_c} F_a^{P1} \\ &\quad - f_{B_c} F_a^{P3} - M_a^{P1} - M_a^{P2}), \end{aligned} \quad (11)$$

where $F(\mathcal{M})$ denotes factorizable (non-factorizable) amplitudes, the subscript $e(a)$ denotes the emission (annihilation) diagrams. The subscript 1(2) denotes the process $B_c^+ \rightarrow D^0\pi^+$ ($B_c^+ \rightarrow D^+\pi^0$), the superscript $T(P)$ denotes amplitudes from the tree (penguin) operators, and f_{B_c} (f_π) is the B_c (π) meson decay constant. The detailed expressions of these amplitudes are shown in Appendix A.

From eq.(10,11), we can see that unlike B^\pm , $B^0(\bar{B}^0)$ decays, we have three kinds of decay amplitudes with

different weak and strong phases: penguin contributions proportional to V_t and two kinds of tree contributions proportional to V_c and V_u , respectively. The interference between them gives large direct CP violation which will be shown later.

As stated in the introduction, the two diagrams in Fig.1 give the contribution for $B_c \rightarrow D$ transition form factor, which is defined as

$$\langle D | d\gamma^\mu b | B_c \rangle = F_+(p_{B_c}^\mu + p_D^\mu) + F_-(p_{B_c}^\mu - p_D^\mu). \quad (12)$$

We calculate F_+ in PQCD and get:

$$\begin{aligned} F_+ = & \frac{4f_B}{\sqrt{2N_c}} \pi C_F M_{B_c}^2 \int_0^1 dx_2 \int_0^\infty b_2 db_2 \phi_D(x_2, b_2) \\ & \times \left\{ [2r_b - x_2 - (r_b - 2x_2)r_2 + (x_2 - 2r_b)r_2^2] \right. \\ & \quad \times \alpha_s(t_e^{(1)}) S_D(t_e^{(1)}) H_{e1}(\alpha_e, \beta_{e1}, b_2) \\ & \quad + [(1 - x_1)r_2(2 - r_2)] \\ & \quad \left. \times \alpha_s(t_e^{(2)}) S_D(t_e^{(2)}) H_{e2}(\alpha_e, \beta_{e2}, b_2) \right\}, \quad (13) \end{aligned}$$

which is the similar expression as F_{e1}^T without Wilson coefficients in the appendix. The numerical results of F_+ can be found in Table I: the form factor F_+ is $0.169_{-0.15}^{+0.05}$ including the uncertainty of ω_D , which is comparable with previous calculations [6, 12].

ω_D	0.40GeV	0.45GeV	0.50GeV
F_+	0.154	0.169	0.174

TABLE I: Form factor F_+ in the different values of ω_D .

C. Input parameters

For D meson wave function, two types of D meson wave function are usually used in the past literature: one is [9]

$$\begin{aligned} \phi_D(x) = & \frac{3}{\sqrt{2N_c}} f_D x(1-x) \{1 + a_D(1-2x)\} \\ & \times \exp\left[-\frac{1}{2}(\omega_D b)^2\right], \quad (14) \end{aligned}$$

in which the last term, $\exp[-\frac{1}{2}(\omega_D b)^2]$, represents the k_T distribution; the other [13, 14] is

$$\phi_D(x) = \frac{3}{\sqrt{2N_c}} f_D x(1-x) \{1 + a_D(1-2x)\}, \quad (15)$$

which is fitted from the measured $B \rightarrow D\ell\nu$ decay spectrum at large recoil. The absence of the last term in the Eq.(14) is due to the insufficiency of the experimental data.

Though the wave function of D meson turns more complicated when it runs at a velocity of about $0.6c$, the light quark's momentum must be less than $p_2^+/2$ because the mass of c quark is by far larger than Λ_{QCD} : $M_c \gg \Lambda_{\text{QCD}}$,

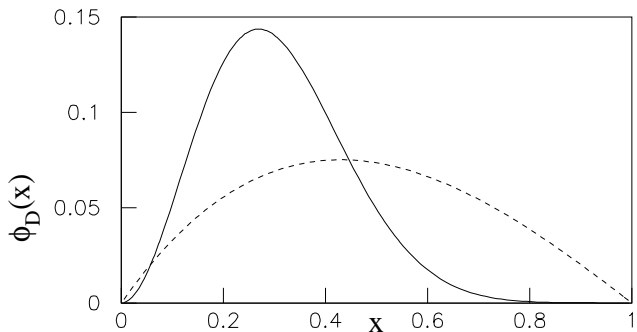


FIG. 5: D meson wave functions: the dashed line for case 1 & 2, the solid line for case 3.

so the wave function of D meson should be strongly suppressed in the region $x_2 > 1/2$ even the k_T contributions are considered. In order to satisfy the above condition, we give up the D wave functions above and construct a new wave function, which also fits the measured $B \rightarrow D\ell\nu$ decay spectrum at large recoil:

$$\begin{aligned} \phi_D(x, b) = & N_D [x(1-x)]^2 \times \\ & \exp\left[-\frac{1}{2}\left(\frac{xM_D}{\omega_D}\right)^2 - \frac{1}{2}(\omega_D)^2 b^2\right], \quad (16) \end{aligned}$$

where N_D is a normalization constant to let

$$\int_0^1 \phi_D(x, b) = \frac{f_D}{2\sqrt{2N_c}}. \quad (17)$$

The behavior of all D meson wave function can be seen in the Fig.5. Our choice of the third case has a broad peak at the small x side, which characterize the mass difference of m_c and m_d .

The π wave functions [15, 16] we adopt are calculated by QCD sum rules and shown in the Appendix B.

The other input parameters are listed below [17, 18]:

$$\begin{aligned} f_{B_c} = 480 \text{ MeV}, \quad f_D = 240 \text{ MeV}, \quad f_\pi = 131 \text{ MeV}, \\ \omega_D = 0.45 \text{ GeV}, \quad M_{0\pi} = 1.60 \text{ GeV}, \quad a_D = 0.3, \\ M_{B_c} = 6.4 \text{ GeV}, \quad M_b = 4.8 \text{ GeV}, \\ M_D = 1.869 \text{ GeV}, \quad M_t = 170 \text{ GeV}, \\ M_W = 80.4 \text{ GeV}, \quad \tau_{B^\pm} = 0.46 \times 10^{-12} \text{ s}, \\ G_F = 1.16639 \times 10^{-5} \text{ GeV}^{-2}. \quad (18) \end{aligned}$$

The CKM parameters used in the paper are:

$$\left| \frac{V_{ub}}{V_{cb}} \right| = 0.085 \pm 0.020, \quad (19)$$

$$|V_{cb}| = 0.039 \pm 0.002, \quad (20)$$

$$R = \left| \frac{V_u}{V_c} \right| = \frac{1 - \lambda^2/2}{\lambda} \left| \frac{V_{ub}}{V_{cb}} \right|. \quad (21)$$

The CKM angle $\phi_3 = \gamma$ is left as a free parameter to discuss CP violation, defined by

$$\gamma = \arg\left(-\frac{V_u}{V_c}\right) = \arg(V_{ub}^*). \quad (22)$$

D. Numerical analysis

We fix $\gamma = 55^\circ$ to discuss the central value of numerical results first.

Both process $B_c^+ \rightarrow D^0\pi^+$ and $B_c^+ \rightarrow D^+\pi^0$ are tree-dominated. The branching ratios and main contributions are give in Table II, from which we can see that the branching ratio of $B_c^+ \rightarrow D^0\pi^+$ is much larger than that of $B_c^+ \rightarrow D^+\pi^0$. Though they are both tree-dominated process, their branching ratios and percentage of different topologies in the whole process are obviously different. Because the annihilation topology give the same contributions to both processes, despite a $\sqrt{2}$ factor, the difference only comes from the emission topology. In the process $B_c^+ \rightarrow D^0\pi^+$, contributions from factorizable emission topology dominate the whole tree contributions for the large Wilson Coefficients $C_2 + C_1/N_c$ in Eq.(A13), which occupy about 93% of total even when the effect of CKM matrix element is considered. ($|\lambda_u| < |\lambda_c|$). On the contrary, contributions from factorizable emission topology in the process $B_c^+ \rightarrow D^+\pi^0$ are suppressed because the Wilson Coefficients C_1 and C_2/N_c in Eq.(A14) cancel each other approximately. From the Table II we also find that contributions from factorizable annihilation topology are at the same order of non-factorizable emission topology.

	$B_c^+ \rightarrow D^0\pi^+$	$B_c^+ \rightarrow D^+\pi^0$
$f_\pi F_c^T$	23.0	0.763
M_e^T	$-0.379 + 0.863i$	$0.854 - 2.16i$
$f_B F_a^T$	$-3.35 + 5.49i$	$-3.35 + 5.49i$
M_a^T	$2.52 - 1.92i$	$2.52 - 1.92i$
$\frac{P}{T_e}$	10%	40%
Br	0.978×10^{-6}	0.196×10^{-6}

TABLE II: Branch ratios and main contributions from tree operators (10^{-3}GeV).

The ratio of the penguin contributions over the tree contributions is about 10% in the process $B_c^+ \rightarrow D^0\pi^+$ and about 40% in the process $B_c^+ \rightarrow D^+\pi^0$ (Table II). The reason for the difference is the following: the term $2r_\pi\phi_\pi^p(x_3)$ in the Eq.(A4) from O_6, O_8 operator contributions, having no factors like x_3 to suppress its integral value in the end-point region and leading to large enhancement compared with other penguin contributions. But the most important reason is that the tree contribution is suppressed in the process $B_c^+ \rightarrow D^+\pi^0$ due to small Wilson coefficients $C_1 + C_2/3$ but not suppressed in the process $B_c^+ \rightarrow D^0\pi^+$. The O_6, O_8 contributions also affect the dependence behavior of the branching ratio and the direct CP asymmetry on the CKM angle γ in the process $B_c^\pm \rightarrow D^\pm\pi^0$, which will be discussed in the following.

The correlation between $Br(B_c^+ \rightarrow D\pi)$ and r_π is shown in Fig.6. Because twist-3 terms of π wave function do not contribute to the form factor (Eq.(A1,A2)), the variation of r_π affects the process $B_c^+ \rightarrow D^+\pi^0$ more heavily than the process $B_c^+ \rightarrow D^0\pi^+$, where the latter

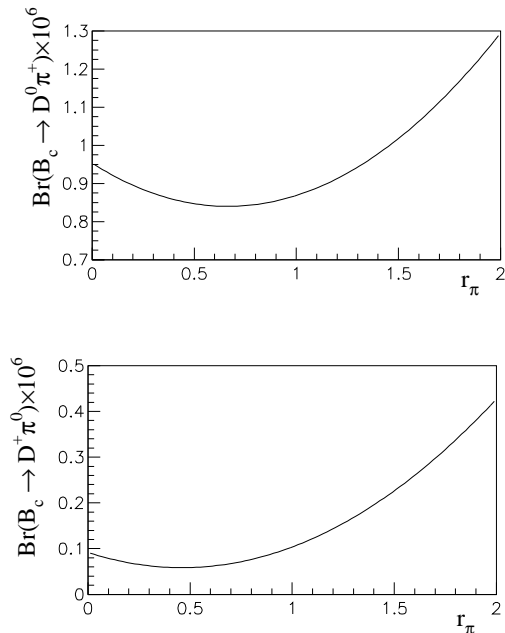


FIG. 6: The correlation between $Br(B_c \rightarrow D\pi)$ and r_π .

dominated by the $B_c \rightarrow D$ form factor diagrams. When $r_\pi = 1.4$, the twist-3 contributions are about 25% in the process $B_c^+ \rightarrow D^0\pi^+$. In the process $B_c^+ \rightarrow D^+\pi^0$, the twist-3 contributions with a relative minus sign cancel some of the twist-2 contributions. When $r_\pi = 1.4$, the branching ratio of $B_c^+ \rightarrow D^+\pi^0$ is about four times of the branching ratio with only twist-2 contributions. When $r_\pi = 0$, the twist-3 contributions vanish and only the contributions from twist-2 terms in the π wave function are left. The corresponding branching ratio is reduced to 0.95×10^{-6} in the process $B_c^+ \rightarrow D^0\pi^+$ and 0.092×10^{-6} in the process $B_c^+ \rightarrow D^+\pi^0$ respectively.

	$B_c^+ \rightarrow D^0\pi^+$	$B_c^+ \rightarrow D^+\pi^0$
$\omega_D = 0.40\text{GeV}$	1.03	0.128
$\omega_D = 0.45\text{GeV}$	0.978	0.196
$\omega_D = 0.50\text{GeV}$	1.19	0.199

TABLE III: Branch ratios in the unit 10^{-6} for different ω_D .

As the only free parameter with large uncertainty, the value of ω_D is the key point to the whole prediction in the calculations of $B_c \rightarrow D\pi$. In the Table III we discuss the branching ratio in three groups of different ω values: $\omega_D = 0.40\text{GeV}$, $\omega_D = 0.45\text{GeV}$ and $\omega_D = 0.50\text{GeV}$, from which we see that the variation of ω_D affects the process $B_c^+ \rightarrow D^0\pi^+$ slightly, but affect the process $B_c^+ \rightarrow D^+\pi^0$ heavily.

According to the CKM parametrization shown in the Eq.(19-22), the decay amplitudes of $B_c \rightarrow D\pi$ can be written as:

$$\begin{aligned}
 M_{D\pi} &= V_u T_u + V_c T_c - V_t P \\
 &= V_u (T_u + P) \left[1 - \frac{1}{R} \frac{T_c + P}{T_u + P} e^{-i\gamma} \right] \\
 &\equiv V_u (T_u + P) \left[1 - z e^{i(-\gamma+\delta)} \right], \quad (23)
 \end{aligned}$$

where $z = \frac{1}{R} \left| \frac{T_c+P}{T_u+P} \right| = \left| \frac{V_c}{V_u} \right| \left| \frac{T_c+P}{T_u+P} \right|$ and the strong phase $\delta = \arg \left(\frac{T_c+P}{T_u+P} \right)$, from our PQCD calculation the numerical value of which is 0.28 and 123° for $B_c^+ \rightarrow D^0\pi^+$, respectively. The emission topology in this channel is only about one time larger than the annihilation topology due to the small CKM factor $|V_u/V_c|$.

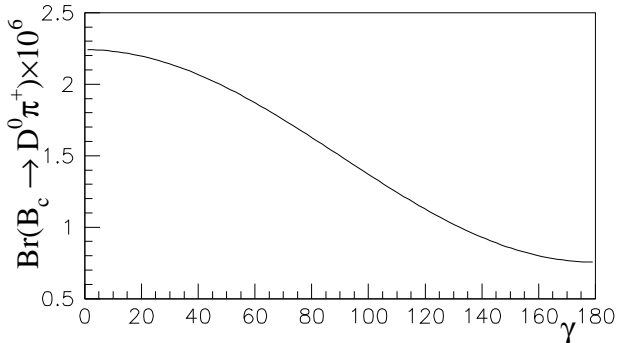


FIG. 7: The correlation between the averaged branching ratio and γ in the process $B_c^\pm \rightarrow D^0\pi^\pm$.

The corresponding conjugate decay of $B_c^+ \rightarrow D\pi$ reads:

$$M_{B_c^- \rightarrow \bar{D}\pi^{-(0)}} = V_u^*(T_u + P) [1 - ze^{i(\gamma+\delta)}] \quad (24)$$

and the averaged branching ratio for $B_c^\pm \rightarrow D^0(\bar{D}^0)\pi^\pm$ reads:

$$\begin{aligned} Br &= \frac{1}{2}(|M|^2 + |\bar{M}|^2) \\ &= \frac{1}{2}|V_u(T_u + P)|^2 [1 - 2z \cos \gamma \cos \delta + z^2], \end{aligned} \quad (25)$$

which is the function of CKM angle γ . Its numerical result depends on γ significantly: the larger γ , the smaller the averaged branching ratio, because $\cos \delta < 0$. The explicit correlation between the averaged branching ratio $B_c^\pm \rightarrow D^0(\bar{D}^0)\pi^\pm$ and γ is shown in the Fig.7.

The direct CP violation A_{cp}^{dir} is defined as

$$A_{cp}^{\text{dir}} = \frac{|M(B_c^+ \rightarrow D^{0(+)}\pi^{+(0)})|^2 - |M(B_c^- \rightarrow D^{0(-)}\pi^{-(0)})|^2}{|M(B_c^+ \rightarrow D^{0(+)}\pi^{+(0)})|^2 + |M(B_c^- \rightarrow D^{0(-)}\pi^{-(0)})|^2}. \quad (26)$$

There are two different tree contributions and one kind of penguin contribution with different strong and weak phases, which will contribute to the CP asymmetry. Using eq.(23,24), A_{cp}^{dir} can be simplified as

$$A_{cp}^{\text{dir}} = -\frac{2z \sin \delta \sin \gamma}{1 - 2z \cos \delta \cos \gamma + z^2}, \quad (27)$$

which is proportional to $\sin \gamma$ approximately. This is shown in Fig.8. When $\gamma = 55^\circ$, the direct CP asymmetry is about -50% in the process $B_c^+ \rightarrow D^0\pi^+$.

The $B_c \rightarrow D^+\pi^0$ becomes a little more complicated: the tree contributions from the emission topology M_e^T (in Table I) is suppressed due to the small Wilson coefficients $C_1 + C_2/3$. In this case, the three different contributions with different weak and strong phases (two

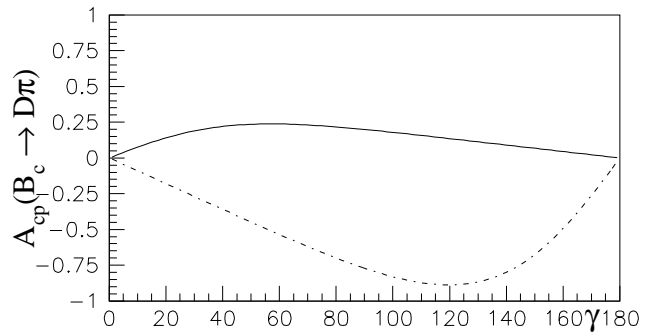


FIG. 8: The correlation between the direct CP violation and γ , the solid line for $B_c^\pm \rightarrow D^\pm\pi^0$ and the dashed line for $B_c^\pm \rightarrow D^0(\bar{D}^0)\pi^\pm$.

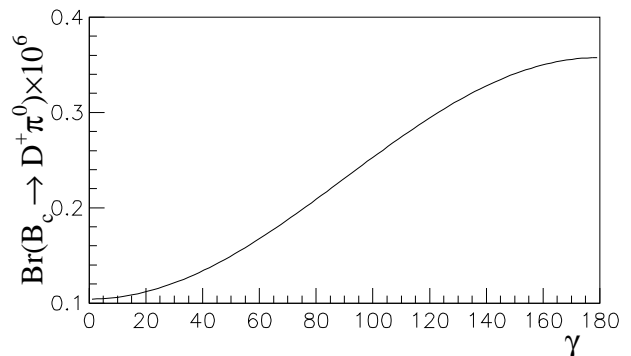


FIG. 9: The correlation between the averaged branching ratio and γ in the process $B_c^\pm \rightarrow D^\pm\pi^0$.

tree contributions and one penguin contributions) are at the same order of magnitude. We can still use Eq.(25) and Eq.(27) to get the behavior of the branching ratio and the direct CP asymmetry on γ . Now the numerical values of z and δ are 3.1 and -20° respectively. Different from the averaged branching ratio of the process $B_c \rightarrow D^+\pi^0$, the averaged branching ratio of the process $B_c \rightarrow D^0\pi^+$ becomes smaller when γ becomes larger because $\cos \delta > 0$. The behavior of the branching ratio and the direct CP asymmetry does not change much, but the shape of the former turns more sharp. In one word, the branching ratio of $B_c^\pm \rightarrow D^\pm\pi^0$ shown in Fig.9 are more sensitive to the value of γ , which is quite different from the case for $B_c^\pm \rightarrow D^0\pi^\pm$, but the direct CP asymmetry of $B_c^\pm \rightarrow D^\pm\pi^0$ shown in Fig.8 does not change greatly because the large uncertainty from γ cancels in the ratio of the direct CP asymmetry. When $\gamma = 55^\circ$, the direct CP asymmetry is about 25% in the process $B_c^\pm \rightarrow D^\pm\pi^0$. As pointed out in ref.[19], the CP asymmetry is sensitive to the next-to-leading order contribution, which is more complicated, the result shown here should be taken carefully.

IV. CONCLUSION

In this paper we discuss the process $B_c \rightarrow D^0\pi^+$ and $B_c \rightarrow D^+\pi^0$ in the PQCD approach and get their branching ratios $1.03_{-0.04}^{+0.16} \times 10^{-6}$ and $1.96_{-0.68}^{+0.03} \times 10^{-7}$ respec-

tively. We also predict the possible large direct CP asymmetry in the two processes: $A_{cp}^{\text{dir}}(B_c^\pm \rightarrow D^0\pi^\pm) \approx -50\%$ and $A_{cp}^{\text{dir}}(B_c^\pm \rightarrow D^\pm\pi^0) \approx 25\%$ when $\gamma = 55^\circ$. The possible theoretical uncertainty are also analyzed. We hope it can be tested in the coming experiments at Tevatron, LHC and the super-B factory.

work is partly supported by National Science Foundation of China.

Acknowledgments

One of the authors (JFC) thank C.H. Chang, Y. Li, Y.-L. Shen and X.-Q. Yu for the beneficial discussions. This

APPENDIX A: CONTRIBUTIONS FROM ALL THE DIAGRAMS

1. Contributions from factorizable diagrams

All diagrams are sorted into two kinds: emission topology and annihilation topology shown in Fig.1,3 and Fig.2,4. The factorizable tree contributions from emission topology read:

$$\begin{aligned}
F_{ei}^{T(P1,P2)} &= \frac{4f_B}{\sqrt{2N_c}} \pi C_F M_{B_c}^2 \int_0^1 dx_2 \int_0^\infty b_2 db_2 \phi_D(x_2, b_2) \\
&\times \left\{ [2r_b - x_2 - (r_b - 2x_2)r_2 + (x_2 - 2r_b)r_2^2] E_{ei}^{T(P1,P2)}(t_e^{(1)}) H_{e1}(\alpha_e, \beta_{e1}, b_2) \right. \\
&\left. + [(1 - x_1)r_2(2 - r_2)] E_{ei}^{T(P1,P2)}(t_e^{(2)}) H_{e2}(\alpha_e, \beta_{e2}, b_2) \right\}, \tag{A1}
\end{aligned}$$

$$\begin{aligned}
F_{ei}^{P3} &= -\frac{8f_B}{\sqrt{2N_c}} r_K \pi C_F M_{B_c}^2 \int_0^1 dx_2 \int_0^\infty b_2 db_2 \phi_D(x_2, b_2) \\
&\times \left\{ [-2 + r_b + (1 - 4r_b + x_2)r_2 + (r_b - 2x_2 + 2)r_2^2] E_{ei}^{P3}(t_e^{(1)}) H_{e1}(\alpha_e, \beta_{e1}, b_2) \right. \\
&\left. - [x_1 + 2(1 - 2x_1)r_2 - (2 - x_1)r_2^2] E_{ei}^{P3}(t_e^{(2)}) H_{e2}(\alpha_e, \beta_{e2}, b_2) \right\}. \tag{A2}
\end{aligned}$$

Because b and c are both massive quarks, there is no collinear divergence in the $B_c \rightarrow D$ transition, so the threshold resummation needn't to be considered. In all the expressions, T denotes the contributions from tree operators, $P1$ denotes the penguin contributions with the Dirac structure $(V - A) \otimes (V - A)$, $P2$ denotes the penguin contributions with the Dirac structure $(V - A) \otimes (V + A)$, and $P3$ denotes the penguin contributions with the Dirac structure $(S - P) \otimes (S + P)$; the subscript $e(a)$ denotes the factorizable emission (annihilation) diagrams, the subscript ne (na) denotes the nonfactorizable emission (annihilation) diagrams.

The factorizable tree contributions from annihilation topology read:

$$\begin{aligned}
F_a^{T(P1)} &= 8\pi C_F M_{B_c}^2 \int_0^1 dx_2 dx_3 \int_0^\infty b_2 db_2 b_3 db_3 \phi_D(x_2, b_2) \\
&\times \left\{ [(x_3 - (1 + 2x_3)r_2^2)\phi_\pi(x_3) + r_2 r_\pi ((1 + 2x_3)\phi_\pi^p(x_3) - (1 - 2x_3)\phi_\pi^\sigma(x_3))] \right. \\
&\quad \times E_a^{T(P1)}(t_a^{(1)}) H_a(\alpha_a, \beta_{a1}, b_2, b_3) S_t(x_3) \\
&\left. - [x_2(1 - r_2^2)\phi_\pi(x_3) + 2r_2 r_\pi (1 + x_2)\phi_\pi^p(x_3)] E_a^{T(P1)}(t_a^{(2)}) H_a(\alpha_a, \beta_{a2}, b_3, b_2) S_t(x_2) \right\}, \tag{A3}
\end{aligned}$$

$$\begin{aligned}
F_a^{P3} &= -16\pi C_F M_{B_c}^2 \int_0^1 dx_2 dx_3 \int_0^\infty b_2 db_2 b_3 db_3 \phi_D(x_2, b_2) \\
&\times \left\{ [-r_2\phi_\pi(x_3) + r_\pi(-x_3 + (2 + x_3)r_2^2)\phi_\pi^p + r_\pi x_3(1 - r_2^2)\phi_\pi^\sigma(x_3)] \right. \\
&\quad \times E_a^{P3}(t_a^{(1)}) H_a(\alpha_a, \beta_{a2}, b_2, b_3) S_t(x_3) \\
&\left. - [x_2 r_2 \phi_\pi(x_3) + 2r_\pi(1 - (1 - x_2)r_2^2)\phi_\pi^p(x_3)] E_a^{P3}(t_a^{(2)}) H_a(\alpha_a, \beta_{a2}, b_3, b_2) S_t(x_2) \right\}, \tag{A4}
\end{aligned}$$

where the factor $S_t(x)$ is the jet function from the threshold resummation [20]:

$$S_t(x) = \frac{2^{1+2c}\Gamma(3/2+c)}{\sqrt{\pi}\Gamma(1+c)} [x(1-x)]^c, \quad c = 0.3. \tag{A5}$$

The factors $E_i^{T(P)}(t)$ contain the Wilson coefficients $a(t)$ at scale t and the evolution from t to the factorization scale $1/b$ in the Sudakov factors $S(t)$:

$$\begin{aligned} E_{ej}^{T(Pi)}(t) &= \alpha_s(t) a_{ej}^{T(Pi)}(t) S_D(t), \\ E_a^{T(Pi)}(t) &= \alpha_s(t) a_{e1}^{T(Pi)}(t) S_D(t) S_\pi(t), \end{aligned} \quad (\text{A6})$$

where $S_D(t), S_\pi(t)$, the Sudakov factors, are defined as

$$S_D(t) = s(x_2 P_2^+, b_2) + 2 \int_{1/b_2}^t \frac{d\mu}{\mu} \gamma_q(\mu), \quad (\text{A7})$$

$$S_\pi(t) = s(x_3 P_3^-, b_3) + s((1-x_3)P_3^-, b_3) + 2 \int_{1/b_3}^t \frac{d\mu}{\mu} \gamma_q(\mu), \quad (\text{A8})$$

and $s(Q, b)$ is given as [21]

$$\begin{aligned} s(Q, b) &= \int_{1/b}^Q \frac{d\mu}{\mu} \left[\left\{ \frac{2}{3}(2\gamma_E - 1 - \ln 2) + C_F \ln \frac{Q}{\mu} \right\} \frac{\alpha_s(\mu)}{\pi} \right. \\ &\quad \left. + \left\{ \frac{67}{9} - \frac{\pi^2}{3} - \frac{10}{27} n_f + \frac{2}{3} \beta_0 \ln \frac{e^{\gamma_E}}{2} \right\} \left(\frac{\alpha_s(\mu)}{\pi} \right)^2 \ln \frac{Q}{\mu} \right], \end{aligned} \quad (\text{A9})$$

where the Euler constant $\gamma_E = 0.57722 \dots$, and $\gamma_q = -\alpha_s/\pi$ is the quark anomalous dimension.

The hard functions H are

$$H_{e1}(\alpha, \beta, b) = \frac{K_0(\alpha b) - K_0(\beta b)}{\beta^2 - \alpha^2}, \quad (\text{A10})$$

$$H_{e2}(\alpha, \beta, b) = \frac{1}{(1-x_1)(x_1-r_2^2)} K_0(\alpha b), \quad (\text{A11})$$

$$H_a(\alpha, \beta, b_1, b_2) = [\theta(b_1 - b_2) K_0(\alpha b_1) I_0(\alpha b_2) + \theta(b_2 - b_1) K_0(\alpha b_2) I_0(\alpha b_1)] K_0(\beta b_2), \quad (\text{A12})$$

where K_0, I_0, H_0 and J_0 are the Bessel functions of order 0. It is implied that the transformed Bessel functions K_0 and I_0 become the corresponding Bessel functions with real variable when their variables are complex.

The Wilson Coefficients a_i read:

$$a_{e1}^T(t) = C_2 + \frac{C_1}{N_c}, \quad (\text{A13})$$

$$a_{e1}^{P1}(t) = C_4 + \frac{C_3}{N_c} + C_{10} + \frac{C_9}{N_c},$$

$$a_{e1}^{P3}(t) = \left(C_6 + \frac{C_5}{N_c} \right) + \left(C_8 + \frac{C_7}{N_c} \right),$$

$$a_{e2}^T(t) = C_1 + \frac{C_2}{N_c}, \quad (\text{A14})$$

$$a_{e2}^{P1}(t) = - \left(C_4 + \frac{C_3}{N_c} \right) + \frac{3}{2} \left(C_9 + \frac{C_{10}}{N_c} \right) + \frac{1}{2} \left(C_{10} + \frac{C_9}{N_c} \right),$$

$$a_{e2}^{P2}(t) = - \frac{3}{2} \left(C_7 + \frac{C_8}{N_c} \right),$$

$$a_{e2}^{P3}(t) = - \left(C_6 + \frac{C_5}{N_c} \right) + \frac{1}{2} \left(C_8 + \frac{C_7}{N_c} \right). \quad (\text{A15})$$

All the Wilson coefficients C_i above should be evaluated at the appropriate scale t . The hard scale t 's are chosen as the maximum of the virtuality of internal momentum transition in the hard amplitudes, including $1/b_i$:

$$t_e^{(1)} = \max(|\alpha_e|, |\beta_{e1}|, 1/b_2),$$

$$t_e^{(2)} = \max(|\alpha_e|, |\beta_{e2}|, 1/b_2),$$

$$t_a^{(1)} = \max(|\beta_{a1}|, 1/b_2, 1/b_3),$$

$$t_a^{(2)} = \max(|\beta_{a2}|, 1/b_2, 1/b_3),$$

where

$$\begin{aligned}
\alpha_e^2 &= (1 - x_1 - x_2)(x_1 - r_2^2)M_{B_c}^2, \\
\beta_{e1}^2 &= [r_b^2 - x_2(1 - r_2^2)]M_{B_c}^2, \\
\beta_{e2}^2 &= (1 - x_1)(x_1 - r_2^2)M_{B_c}^2, \\
\alpha_a^2 &= -x_2x_3M_{B_c}^2(1 - r_2^2), \\
\beta_{a1}^2 &= -x_3M_{B_c}^2(1 - r_2^2), \\
\beta_{a2}^2 &= -x_2M_{B_c}^2(1 - r_2^2).
\end{aligned} \tag{A16}$$

2. Contributions from non-factorizable diagrams

Different from factorizable diagrams, non-factorizable diagrams include convolution of all three wave functions and, of course, the convolution of Sudakov factors. Their amplitudes are:

$$\begin{aligned}
M_{ei}^{T(P1)} &= \frac{8}{N_c} \pi C_F f_B M_{B_c}^2 \int_0^1 dx_2 dx_3 \int_0^\infty b_2 db_2 b_3 db_3 \phi_D(x_2, b_2) \phi_\pi(x_3) \\
&\times \left\{ [1 - x_1 - x_3 - (1 - x_1 - x_2)r_2 - (x_2 - 2x_3)r_2^2] E_{ne\ i}^{T(P1)}(t_a^{(1)}) H_a(\alpha_{ne}, \beta_{ne1}, b_2, b_3) \right. \\
&\left. + [(2x_1 + x_2 - x_3 - 1) + (1 - x_1 - x_2)r_2 + (-2x_1 - x_2 + 2x_3)r_2^2] E_{ne\ i}^{T(P1)}(t_a^{(2)}) H_a(\alpha_{ne}, \beta_{ne2}, b_2, b_3) \right\}, \tag{A17}
\end{aligned}$$

$$\begin{aligned}
M_{ei}^{P2} &= \frac{8}{N_c} \pi r_\pi C_F f_B M_{B_c}^2 \int_0^1 dx_2 dx_3 \int_0^\infty b_2 db_2 b_3 db_3 \phi_D(x_2, b_2) \\
&\times \left\{ [(1 - x_1 - x_3 + (2 - 2x_1 - x_2 - x_3)r_2 + (1 - x_1 - x_2 + x_3)r_2^2)] \phi_\pi^p(x_3) \right. \\
&\quad + (1 - x_1 - x_3 + (x_2 - x_3)r_2 + (-1 + x_1 + x_2 + x_3)r_2^2) \phi_\pi^\sigma(x_3) \left. \right] E_{ne\ i}^{P2}(t_a^{(1)}) H_a(\alpha_{ne}, \beta_{ne1}, b_2, b_3) \\
&\left. + [(x_1 - x_3 + (2x_1 + x_2 - x_3 - 1)r_2 + (x_1 + x_2 + x_3 - 2)r_2^2)] \phi_\pi^p(x_3) \right. \\
&\quad \left. + (-x_1 + x_3 + (x_2 + x_3 - 1)r_2 + (x_1 + x_2 - x_3)r_2^2) \phi_\pi^\sigma(x_3) \right] E_{ne\ i}^{P2}(t_a^{(2)}) H_a(\alpha_{ne}, \beta_{ne2}, b_2, b_3) \left. \right\}, \tag{A18}
\end{aligned}$$

$$\begin{aligned}
M_{ei}^{P3} &= \frac{8}{N_c} \pi C_F f_B M_{B_c}^2 \int_0^1 dx_2 dx_3 \int_0^\infty b_2 db_2 b_3 db_3 \phi_D(x_2, b_2) \phi_\pi(x_3) \\
&\times \left\{ [-2 + 2x_1 + x_2 + x_3 + (1 - x_1 - x_2)r_2 + (2 - 2x_1 - x_2 - 2x_3)r_2^2] E_{ne\ i}^{P3}(t_a^{(1)}) H_a(\alpha_{ne}, \beta_{ne1}, b_2, b_3) \right. \\
&\left. + [-x_1 + x_3 + (x_1 + x_2 - 1)r_2 - (x_2 + 2x_3 - 2)r_2^2] E_{ne\ i}^{P3}(t_a^{(2)}) H_a(\alpha_{ne}, \beta_{ne2}, b_2, b_3) \right\}, \tag{A19}
\end{aligned}$$

$$\begin{aligned}
M_a^{T(P1)} &= \frac{8}{N_c} \pi C_F f_B M_{B_c}^2 \int_0^1 dx_2 dx_3 \int_0^\infty b_2 db_2 b_3 db_3 \phi_D(x_2, b_2) \\
&\times \left\{ [(-x_1 + x_2 + r_2) \phi_\pi(x_3) + (-2x_1 + x_2 + x_3 + 4r_2)r_2 r_\pi \phi_\pi^p(x_3) + (x_2 - x_3)r_2 r_\pi \phi_\pi^\sigma(x_3)] \right. \\
&\quad \times E_{ne1}^{T(P1)}(t_{na}^{(1)}) H_{na}(\alpha_{na}, \beta_{na1}, b_2) \\
&\quad + [(1 - x_1 - x_3 - r_b + (-x_2 + 2x_3 + r_b)r_2^2) \phi_\pi(x_3) + (2 - 2x_1 - x_2 - x_3 - 4r_b)r_2 r_\pi \phi_\pi^p(x_3) \\
&\quad \left. + (x_2 - x_3)r_2 r_\pi \phi_\pi^\sigma(x_3)] E_{ne1}^{T(P1)}(t_{na}^{(2)}) H_{na}(\alpha_{na}, \beta_{na2}, b_2) \right\}, \tag{A20}
\end{aligned}$$

$$\begin{aligned}
M_a^{P2} &= -\frac{8}{N_c} \pi C_F f_B M_{B_c}^2 \int_0^1 dx_2 dx_3 \int_0^\infty b_2 db_2 b_3 db_3 \phi_D(x_2, b_2) \\
&\times \left\{ [(-x_1 + x_2 - r_2)r_2 \phi_\pi(x_3) + (x_1 - x_3 + r_2 + (x_1 - x_2 + x_3)r_2^2) r_\pi \phi_\pi^p(x_3) \right. \\
&\quad + (x_1 + x_2 - x_3 + (-x_1 + x_2 + x_3)r_2^2) r_\pi \phi_\pi^\sigma(x_3)] E_{ne1}^{P2}(t_{na}^{(1)}) H_{na}(\alpha_{na}, \beta_{na1}, b_2) \\
&\left. - [(-1 - r_b + x_1 + x_2)r_2 \phi_\pi(x_3) + (1 + r_b - x_1 - x_3 + (1 + r_b - x_1 - x_2 + x_3)r_2^2) r_\pi \phi_\pi^p(x_3) \right. \\
&\quad \left. + (1 + r_b - x_1 - x_3 + (-1 - r_b + x_1 + x_2 + x_3)r_2^2) r_\pi \phi_\pi^\sigma(x_3)] E_{ne1}^{P2}(t_{na}^{(2)}) H_{na}(\alpha_{na}, \beta_{na2}, b_2) \right\}. \tag{A21}
\end{aligned}$$

where the hard kernel H_{na} is defined as

$$H_{na}(\alpha, \beta, b) = \frac{K_0(\alpha b) - K_0(\beta b)}{\beta^2 - \alpha^2}, \tag{A22}$$

and the factor $E(t)$ turns into:

$$E_{nej}^{T(Pi)}(t) = \alpha_s(t) a_{nej}^{T(Pi)}(t) S_D(t) S_\pi(t), \quad (\text{A23})$$

where the Wilson coefficients a read:

$$\begin{aligned} a_{ne1}^T(t) &= C_1, \\ a_{ne1}^{P1}(t) &= C_3 + C_9, \\ a_{ne1}^{P2}(t) &= C_5 + C_7, \\ a_{ne2}^T(t) &= C_2, \\ a_{ne2}^{P1}(t) &= -C_3 + \frac{1}{2}C_9 + \frac{3}{2}C_{10}, \\ a_{ne2}^{P2}(t) &= -C_5 + \frac{1}{2}C_7, \\ a_{ne2}^{P3}(t) &= \frac{3}{2}C_8. \end{aligned} \quad (\text{A24})$$

The hard scale t 's are chosen as the maximum of the virtuality of internal momentum transition in the hard amplitudes, including $1/b_i$:

$$\begin{aligned} t_e^{(1)} &= \max(|\alpha_{ne}|, |\beta_{ne1}|, 1/b_2, 1/b_3), \\ t_e^{(2)} &= \max(|\alpha_{ne}|, |\beta_{ne2}|, 1/b_2, 1/b_3), \\ t_a^{(1)} &= \max(|\alpha_{na}|, |\beta_{na1}|, 1/b_2), \\ t_a^{(1)} &= \max(|\alpha_{na}|, |\beta_{na2}|, 1/b_2), \end{aligned}$$

where

$$\begin{aligned} \alpha_e^2 &= (1 - x_1 - x_2)(x_1 - r_2^2) M_{B_c}^2, \\ \beta_{ne1} &= -(1 - x_1 - x_2) [(1 - x_3)(1 - r_2^2) - x_1 + r_2^2] M_{B_c}^2, \\ \beta_{ne2} &= -(1 - x_1 - x_2) [x_3(1 - r_2^2) - x_1 + r_2^2] M_{B_c}^2, \\ \alpha_a^2 &= -x_2 x_3 M_{B_c}^2 (1 - r_2^2), \\ \beta_{na1} &= x_1 [x_2 + x_3(1 - r_2^2)] M_{B_c}^2, \\ \beta_{na2} &= (1 - x_1) [x_2 + x_3(1 - r_2^2)] M_{B_c}^2. \end{aligned} \quad (\text{A25})$$

APPENDIX B: THE π MESON WAVE FUNCTIONS

The different distribution amplitudes of π meson wave functions are given as [15, 16]

$$\phi_\pi(x) = \frac{3}{\sqrt{6}} f_\pi x(1-x) \left[1 + 0.44 C_2^{3/2}(2x-1) + 0.25 C_4^{3/2}(2x-1) \right], \quad (\text{B1})$$

$$\phi_\pi^p(x) = \frac{f_\pi}{2\sqrt{6}} \left[1 + 0.43 C_2^{1/2}(2x-1) + 0.09 C_4^{1/2}(2x-1) \right], \quad (\text{B2})$$

$$\phi_\pi^\sigma(x) = \frac{f_\pi}{2\sqrt{6}} (1-2x) \left[1 + 0.55(10x^2 - 10x + 1) \right]. \quad (\text{B3})$$

with the Gegenbauer polynomials

$$\begin{aligned} C_2^{1/2}(t) &= \frac{1}{2}(3t^2 - 1), & C_4^{1/2}(t) &= \frac{1}{8}(35t^4 - 30t^2 + 3), \\ C_2^{3/2}(t) &= \frac{3}{2}(5t^2 - 1), & C_4^{3/2}(t) &= \frac{15}{8}(21t^4 - 14t^2 + 1). \end{aligned} \quad (\text{B4})$$

[1] CDF collaboration, F. Abe, *et al.*, Phys. Rev. D **58**, 112004 (1998).

[2] Y. Y. Keum, H. N. Li and A. I. Sanda, Phys. Rev. D **63**,

- 054008 (2001); C. H. Chen, Y. Y. Keum and H. n. Li, Phys. Rev. D **64**, 112002 (2001); Y. Y. Charng and H. n. Li, arXiv:hep-ph/0308257.
- [3] C.-D. Lü, K. Ukai and M.-Z. Yang, Phys. Rev. D **63**, 074009 (2001); C.-D. Lü, pp. 173-184, Proceedings of International Conference on Flavor Physics (ICFP 2001), World Scientific, 2001, hep-ph/0110327.
- [4] M. Beneke, G. Buchalla, M. Neubert and C. T. Sachrajda, Phys. Rev. Lett. **83**, 1914 (1999); Nucl. Phys. B **606**, 245 (2001); M. Beneke and M. Neubert, Nucl. Phys. B **675**, 333 (2003).
- [5] C.W. Bauer, D. Pirjol, I.W. Stewart, Phys. Rev. Lett. **87**, 201806 (2001); Phys. Rev. D **65**, 054022 (2002); C.W. Bauer, I.W. Stewart, Phys. Lett. B **516**, 134 (2001); Phys. Lett. B **516**, 134 (2001); Phys. Rev. D **65**, 054022 (2002).
- [6] D. Du and Z. Wang, Phys. Rev. D **39**, 1342 (1989);
- [7] J.Schwinger, Phys. Rev. Lett. **12**, 630 (1965); M.Bauer and B. Stech, Phys. Lett. **B152**, 380 (1985); M.Bauer, B. Stech and M. Wirbel, Z. Phys. **C34**, 103 (1987).
- [8] A. Ali and C. Greub, Phys. Rev. **D57**, 2996 (1998); A. Ali, J.Chay, C. Greub and P. Ko, Phys. Lett. **B424**, 161 (1998); A. Ali, G. Kramer and C. D. Lü, Phys. Rev. **D58**, 094009 (1998); Y.-H. Chen, H.-Y. Cheng, B. Tseng, K.-C. Yang, Phys. Rev. D **60** 094014 (1999).
- [9] T. Kurimoto, H.-n. Li, and A. I. Sanda, Phys. Rev. D **67**, 054028 (2003).
- [10] C.D. Lü and M.Z. Yang, Eur. Phys. J. C **28**, 515 (2003).
- [11] G. Buchalla, A.J. Buras and M.E. Lautenbacher, Rev. Mod. Phys. **68**, 1125 (1996).
- [12] J.F. Liu and K.T. Chao, Phys. Rev. D **56**, 4133 (1997); C.Q. Geng, C.W. Hwang and C.C. Liu, Phys. Rev. D **65**, 094037 (2002).
- [13] Y.-Y. Keum, T. Kurimoto, H.-N. Li, C.-D. Lü, A.I. Sanda, Phys. Rev. D **69**, 094018 (2004).
- [14] G.-L. Song and C.-D. Lü, Phys. Rev. D **70**, 034006 (2004).
- [15] P. Ball, JHEP, **09**, 005, (1998); JHEP, **01**, 010, (1999).
- [16] P. Ball, V.M. Braun, Y. Koike, and K. Tanaka, Nucl. Phys. B **529**, 323 (1998); P. Ball, V. M. Braun, hep-ph/9808229.
- [17] C.-H. Chang and Y.Q. Chen, Phys. Rev. D **49**, 3399 (1994).
- [18] Particle Data Group, Phys. Rev. D **66**, Part I (2002).
- [19] H.-n. Li, S. Mishima, A.I. Sanda, hep-ph/0508041.
- [20] H.n. Li, Phys. Rev. D **66**, 094010 (2002).
- [21] H.-n. Li, B. Melic, Eur. Phys. J. C **11**, 695 (1999).

